Published in final edited form as:
Cell Metab. 2011 June 8; 13(6): 729–738. doi:10.1016/j.cmet.2011.03.019.

FGF15/19 Regulates Hepatic Glucose Metabolism By Inhibiting the CREB-PGC-1α Pathway

Matthew J. Potthoff[1,3,4,‡], **Jamie Boney-Montoya**[2,‡], **Mihwa Choi**[2], **Tianteng He**[3], **Nishanth E. Sunny**[3], **Santhosh Satapati**[3], **Kelly Suino-Powell**[5], **H. Eric Xu**[5], **Robert D. Gerard**[2], **Brian N. Finck**[6,7], **Shawn C. Burgess**[1,3], **David J. Mangelsdorf**[1,4,*], and **Steven A. Kliewer**[1,2,*]

[1]Department of Pharmacology, University of Texas Southwestern Medical Center, Dallas, Texas 75390-9148, USA

[2]Department of Molecular Biology, University of Texas Southwestern Medical Center, Dallas, Texas 75390-9148, USA

[3]Department of Advanced Imaging Center, University of Texas Southwestern Medical Center, Dallas, Texas 75390-9148, USA

[4]Department of Howard Hughes Medical Institute, University of Texas Southwestern Medical Center, Dallas, Texas 75390-9148, USA

[5]Laboratory of Structural Sciences, Van Andel Research Institute, 333 Bostwick Avenue, Grand Rapids, Michigan 49503, USA

[6]Center for Cardiovascular Research, Washington University School of Medicine, St. Louis, Missouri 63110 USA

[7]Center for Human Nutrition, Department of Medicine, Washington University School of Medicine, St. Louis, Missouri 63110 USA

Summary

Regulation of hepatic carbohydrate homeostasis is crucial for maintaining energy balance in the face of fluctuating nutrient availability. Here, we show that the hormone fibroblast growth factor 15/19 (FGF15/19), which is released postprandially from the small intestine, inhibits hepatic gluconeogenesis, like insulin. However, unlike insulin, which peaks in serum 15 minutes after feeding, FGF15/19 expression peaks approximately 45 min later, when bile acid concentrations increase in the small intestine. FGF15/19 blocks the expression of genes involved in gluconeogenesis through a mechanism involving the dephosphorylation and inactivation of the transcription factor cAMP regulatory element binding protein (CREB). This in turn blunts expression of peroxisome proliferator-activated receptor γ coactivator-1α (PGC-1α) and other genes involved in hepatic metabolism. Overexpression of PGC-1α blocks the inhibitory effect of FGF15/19 on gluconeogenic gene expression. These results demonstrate that FGF15/19 works subsequent to insulin as a postprandial regulator of hepatic carbohydrate homeostasis.

*Corresponding authors davo.mango@utsouthwestern.edu, steven.kliewer@utsouthwestern.edu.
‡equal contributions

Supplemental Information
Supplemental Information includes Supplemental Experimental Procedures and three figures and can be found with this article online.

Introduction

Insulin and glucagon have well established roles in controlling substrate utilization and energy balance during the fed and fasted states, respectively. More recently, human fibroblast growth factor (FGF) 19 and its mouse ortholog, FGF15, were identified as metabolic hormones (Fu et al., 2004; Inagaki et al., 2005; Tomlinson et al., 2002). (We will refer to the hormone as FGF15/19 unless specifically referring to the mouse FGF15 or human FGF19 orthologs.) FGF15/19 is an atypical FGF that lacks the conventional heparin-binding domain found in most other FGFs (Goetz et al., 2007). As a consequence, FGF15/19 circulates as a hormone and signals through a cell-surface receptor comprised of classical FGF receptors (FGFRs) complexed with β-Klotho, a membrane-spanning protein (Kurosu et al., 2007; Lin et al., 2007; Wu et al., 2007). FGF15/19 preferentially binds and activates the FGFR4/β-Klotho complex.

FGF15/19 is a postprandial hormone whose expression is induced in the small intestine by bile acids acting through the nuclear bile acid receptor, FXR (Inagaki et al., 2005). In humans, FGF19 plasma concentrations peak 2–3 hr after feeding (Lundasen et al., 2006; Walters et al., 2009). FGF15/19 circulates to repress bile acid synthesis in liver and to promote gallbladder filling (Choi et al., 2006; Holt et al., 2003; Inagaki et al., 2005; Lundasen et al., 2006). FGF15/19 also has broader effects on energy homeostasis. Transgenic mice expressing FGF19 in muscle have a higher basal metabolic rate and are resistant to high fat diet-induced weight gain (Tomlinson et al., 2002). These mice also have lower serum glucose and insulin levels and enhanced insulin sensitivity. Administration of recombinant FGF19 had similar metabolic effects in *db/db* and diet-induced obese mice (Fu et al., 2004).

cAMP regulatory element binding protein (CREB) is a transcription factor that is activated by a diverse array of extracellular signals (Goldman et al., 1997; Mayr and Montminy, 2001). In liver, CREB regulates metabolism in response to fasting. Glucagon and catecholamines activate CREB through protein kinase A, which phosphorylates CREB at Ser133, thereby promoting its interaction with transcriptional coactivator proteins such as CREB-binding protein (CBP) and p300 (Chrivia et al., 1993; Gonzalez and Montminy, 1989; Kwok et al., 1994). Glucagon also causes dephosphorylation of CREB-regulated transcription coactivator 2 (CRTC2), which translocates into the nucleus, where it binds and activates CREB (Bittinger et al., 2004; Koo et al., 2005; Screaton et al., 2004). Among the genes induced by CREB during fasting is peroxisome proliferator-activated receptor γ coactivator protein-1α (PGC-1α) (Herzig et al., 2001), which encodes a transcriptional coactivator protein that interacts with various DNA-binding transcription factors to stimulate the expression of genes involved in gluconeogenesis, fatty acid oxidation, tricarboxylic acid (TCA) cycle flux and mitochondrial oxidative phosphorylation (Burgess et al., 2006; Finck and Kelly, 2006; Handschin and Spiegelman, 2006; Puigserver and Spiegelman, 2003). Overexpression of PGC-1α in CREB-deficient mice restores gluconeogenic gene expression and glucose homeostasis (Herzig et al., 2001).

In this report, we investigated the effects of FGF15/19 on hepatic metabolism. We show that FGF15/19 inhibits gluconeogenesis through a mechanism involving the dephosphorylation and inactivation of CREB and suppression of PGC-1α expression.

Results

FGF15/19 represses PGC-1α and its target genes in liver

To characterize the *in vivo* actions of FGF15/19, we performed gene expression profiling using liver from fasted wild-type mice treated with either vehicle, FGF15 or FGF19 for 6 hr.

As expected for orthologous proteins, FGF15 and FGF19 showed a strong overlap (R^2 = 0.73) in the genes that they regulate (Supplemental Fig. S1A). As expected, FGF15 and FGF19 both suppressed mRNA expression of the bile acid synthesizing enzyme, *Cyp7a1* (Fig. 1A) (Holt et al., 2003; Inagaki et al., 2005). Interestingly, one of the most strongly down-regulated genes in FGF15/19 treated livers was *Pgc1α* (Fig. 1A). There were corresponding decreases in PGC-1α protein (Fig. 1B) and the PGC-1α target genes glucose-6-phosphatase (*G6Pase*), phosphoenolpyruvate carboxykinase (*Pepck*), β-subunit of ATP synthase (*Atp5b*), cytochrome c (*Cytc*) and isocitrate dehydrogenase (*Idh3a*), which encode proteins involved in gluconeogenesis, mitochondrial oxidative phosphorylation and TCA cycle flux (Fig. 1A). Peroxisome proliferator-activated receptor-gamma coactivator-1β (*Pgc1*β) was also down regulated by FGF15/19 (Fig. 1A) as reported (Bhatnagar et al., 2009). These results demonstrate that FGF15/19 regulates the expression of genes involved in gluconeogenesis and fatty acid oxidation. FGF15/19 did not alter expression of fatty acid synthase, steroyl CoA desaturase 1 and acetyl-CoA carboxylase, suggesting that lipogenesis was unaffected (Supplemental Fig. S1B).

To determine the kinetics with which FGF19 regulates gene expression, wild-type mice were fasted overnight to induce gluconeogenesis, administered FGF19 and then sacrificed over a 6 hr time course. *Cyp7a1* mRNA levels were reduced within 4 hr of FGF19 treatment (Fig. 1C). Likewise, *Pgc1α*, *Pepck*, and *G6pase* mRNAs were significantly reduced at the 4 and 6 hr time points (Fig. 1C).

We next examined the relative timing of FGF15 and insulin action following a fasting-refeeding regimen. Wild-type mice were fasted for 24 hr and then gavaged with a high carbohydrate/high fat liquid diet. Plasma insulin (Fig. 1D) and glucose levels (Fig. 1E) peaked sharply within 15 min after refeeding as did liver levels of phosphorylated Akt (Fig. 1F), a measure of insulin action. For technical reasons we are unable to directly measure circulating FGF15 concentrations. As surrogates, we measured *Fgf15* mRNA in ileum and phosphorylation of ERK1/2 in liver, which is stimulated by FGF15/19 (Kurosu et al., 2007). *Fgf15* mRNA levels increased gradually in the ileum, peaking around 1 hr post-gavage (Fig. 1D). ERK1/2 phosphorylation in liver showed a very similar profile (Fig. 1F). These data indicate that postprandial FGF15 levels and signaling activity peak after those of insulin and are consistent with serum FGF19 concentrations in humans peaking 2–3 hr following a meal, well after insulin levels decrease (Lundasen et al., 2006; Walters et al., 2009). Plasma glucagon concentrations decreased only modestly after refeeding (Fig. 1E), which is not surprising given that glucagon levels are already low following a 24 hr fast (Ahren and Havel, 1999; Parker et al., 2002). CREB phosphorylation was reduced within 15 min of refeeding, remained relatively low at the 30 and 60 min time points and then increased (Fig. 1F), suggesting that insulin and FGF15 suppress CREB activity (see below).

We next used loss-of-function and gain-of-function studies to determine whether PGC-1α is required for FGF15/19-mediated repression of gluconeogenic gene expression. For loss-of-function studies, floxed PGC-1α mice (PGC-1$\alpha^{fl/fl}$) (Lin et al., 2004) were administered either control adenovirus (Ad-Con) or a Cre recombinase-expressing adenovirus (Ad-Cre) to eliminate PGC-1α in liver. Groups of PGC-1$\alpha^{fl/fl}$;Ad-Con and PGC-1$\alpha^{fl/fl}$;Ad-Cre mice were subsequently fasted and administered either vehicle or FGF19. PGC-1$\alpha^{fl/fl}$;Ad-Cre mice had the expected reduction in *Pgc1α* mRNA in liver and also had reduced basal expression of *G6Pase* and *Pepck* (Fig. 2A). As expected, FGF19 repressed expression of *Pgc1α*, *G6pase*, *Pepck* and *Cyp7a1* in PGC-1$\alpha^{fl/fl}$;Ad-Con mice. However, the repressive effect of FGF19 on *G6pase* and *Pepck* was lost in PGC-1$\alpha^{fl/fl}$;Ad-Cre mice (Fig. 2A). In contrast, FGF19-mediated repression of *Cyp7a1* occurred in PGC-1$\alpha^{fl/fl}$;Ad-Cre mice, although basal *Cyp7a1* mRNA levels increased in the absence of PGC-1α (Fig. 2A). Thus,

FGF19-mediated repression of PGC-1α is important for the regulation of genes involved in carbohydrate metabolism but not bile acid metabolism.

In complementary gain-of-function studies, wild-type mice were infected with either Ad-Con or a PGC-1α-expressing adenovirus (Ad-PGC-1α). Ad-PGC-1α caused a 15- to 20-fold increase in hepatic *Pgc1α* mRNA but did not further increase basal *G6pase* and *Pepck* expression under these fasted conditions (Fig. 2B). Subgroups of these mice were either infected with an FGF15-expressing adenovirus (Ad-FGF15) or administered FGF19. As expected, FGF15 and FGF19 repressed *Pgc1α*, *G6pase* and *Pepck* in Ad-Con mice (Fig. 2B). However, under conditions of PGC-1α overexpression, neither FGF15 nor FGF19 repressed *G6pase* or *Pepck* (Fig. 2B). Taken together, the loss-of-function and gain-of-function data demonstrate that the effects of FGF15/19 on metabolic gene expression are mediated via regulation of PGC-1α.

The orphan nuclear receptor, small heterodimer partner (SHP), is required for FGF15/19-mediated repression of *Cyp7a1* (Inagaki et al., 2005). To determine whether SHP contributes to FGF19-mediated repression of gluconeogenic gene expression, wild-type and SHP-KO mice were administered vehicle or FGF19, and hepatic gene expression was measured. Unlike *Cyp7a1*, repression of *Pgc1α*, *G6pase* and *Pepck* expression was maintained in both wild-type and SHP-KO mice (Fig. 2C). Thus, FGF19-mediated repression of gluconeogenic genes does not require SHP.

FGF15/19 represses gluconeogenesis

To determine whether the FGF15/19-mediated changes in hepatic gene expression are accompanied by corresponding changes in metabolism, metabolic flux was measured by $^{2}H/^{13}C$ nuclear magnetic resonance (NMR) isotopomer analysis in perfused livers isolated from mice infected with either FGF15-expressing or control adenoviruses. As expected, *Pgc1α, G6pase*, *Pepck*, *Atp5b*, *Cytc*, *Idh3a* and *Cyp7a1* were significantly reduced in liver from mice administered Ad-FGF15 (Fig. 3A). Consistent with these gene expression data, hepatic gluconeogenesis, TCA cycle flux and β-oxidation were significantly reduced and ketogenesis trended lower in liver exposed to FGF15 (Fig. 3B). In experiments performed in parallel, adenoviral expression of FGF15 significantly decreased plasma glucose concentrations and caused downward trends in insulin and ketone body levels but did not affect plasma glucagon concentrations (Fig. 3C). In complementary experiments, more acute administration of recombinant FGF19 did not significantly alter plasma glucagon or insulin levels (Supplemental Fig. S2A and B). Consistent with decreased *Cyp7a1* expression, hepatic cholesterol levels were significantly increased in mice infected with the FGF15-expressing adenovirus (Fig. 3C). Both plasma and hepatic triglyceride concentrations trended lower in response to FGF15 (Supplemental Fig. S2C and D), which is surprising in light of the effect FGF15 has on hepatic β-oxidation. In related experiments, acute FGF19 administration had no effect on hepatic triglyceride concentrations (Supplemental Fig. S2E), and FGF15-KO mice showed no change in hepatic triglyceride concentrations compared to wild-type mice (Supplemental Fig. S2F). These paradoxical results may be the consequence of FGF15/19 also acting on tissues other than liver. Taken together, these NMR isotopomer and metabolic parameter data demonstrate that FGF15/19 suppresses several hepatic metabolic pathways, including gluconeogenesis, TCA cycle flux and fatty acid oxidation, which are induced during fasting.

To determine whether FGF15/19-mediated repression of gluconeogenic gene expression might be an indirect consequence of increased insulin sensitivity, insulin tolerance tests (ITT) were performed in mice administered either vehicle or FGF19, or mice administered control or FGF15-expressing adenovirus. In both experiments, mice treated with FGF19 or FGF15 exhibited similar insulin sensitivity compared to their respective controls

(Supplemental Fig. S2G and H). To further test whether FGF19 improves hepatic insulin sensitivity, hyperinsulinemic/euglycemic clamps were performed. Consistent with the ITT results, mice administered FGF19 demonstrated equivalent sensitivity to insulin as vehicle-treated animals (Supplemental Fig. S2I and J). Thus, FGF15/19 does not improve insulin sensitivity in lean mice.

FGF15-KO and FGFR4-KO mice were used to directly assess the physiologic relevance of the FGF15/19-FGFR4 pathway in regulating gluconeogenesis. *Pgc1α*, *Pepck* and *G6pase* mRNA levels were significantly elevated in liver from fed FGF15-KO and FGFR4-KO mice (Fig. 3D and E). To determine whether these changes in gene expression corresponded with increased gluconeogenesis, we performed a modified pyruvate/lactate challenge using uniformly labeled ^{13}C pyruvate and lactate in fed wild-type and FGF15-KO mice. Intraperitoneal (i.p.) administration of pyruvate/lactate caused a significantly greater increase in plasma glucose levels in FGF15-KO mice compared to wild-type mice (Fig. 3F). Mass spectrometry analysis verified that the additional plasma glucose was derived from labeled substrate (Fig. 3G). Taken together, these data demonstrate that FGF15 contributes to the repression of gluconeogenesis in the fed state.

To further examine the physiological consequences of FGF15 and FGFR4 deficiency, FGF15-KO and FGFR4-KO mice and their wild-type counterparts were fasted 24 hrs, fed a high carbohydrate/high fat liquid diet by oral gavage, and their blood glucose levels analyzed over time. Blood glucose levels were elevated significantly in the FGF15-KO mice at the 1 and 2 hr time points (Fig. 3H) and in the FGFR4-KO mice at the 2 hr time point (Fig. 3I), indicating an impaired postprandial response when the FGF15-FGFR4 pathway is disrupted. Plasma insulin levels were not significantly altered in either FGF15-KO or FGFR4-KO mice although there was a trend toward decreased plasma insulin concentrations in the FGFR4-KO mice (Fig. 3J and K). ITT in FGF15-KO and FGFR4-KO mice revealed no changes in insulin sensitivity (Supplemental Fig. S2K and L). In addition, plasma glucagon levels did not differ between wild-type and FGF15-KO mice (Supplemental Fig. S2M). Thus, the FGF15-FGFR4 pathway modulates postprandial carbohydrate homeostasis without affecting insulin sensitivity or glucagon concentrations.

FGF15/19 Represses CREB

To gain insight into how FGF15/19 represses *Pgc1α*, we analyzed candidate signaling pathways for activation by FGF19 *in vivo*. Fasted wild-type and FGFR4-KO mice were administered FGF19 or vehicle for 30 min and multiple phosphorylation cascades analyzed. As expected, administration of FGF19 increased FRS2α and ERK1/2 phosphorylation in liver of wild-type but not FGFR4-KO mice (Fig. 4A). FGF19 had no effect on the phosphorylation of either Akt or FOXO1. However, FGF19 caused a marked reduction in the phosphorylation of CREB at Ser133, a site that regulates CREB transcriptional activity (Gonzalez and Montminy, 1989), in wild-type but not FGFR4-KO mice (Fig. 4A).

Since CREB induces *Pgc1α* by binding to a cAMP response element (CRE) in the *Pgc1α* promoter and recruiting coactivator proteins such as CBP (Herzig et al., 2001), we performed chromatin immunoprecipitation (ChIP) analysis for CREB and CBP using liver from mice treated with vehicle or FGF19. Administration of FGF19 reduced CREB and CBP binding to the *Pgc1α* promoter (Fig. 4B). CREB and CBP binding were also reduced in liver from mice infected with an FGF15-expressing adenovirus (Fig. 4C). These data indicate that FGF15/19 inhibits *Pgc1α* expression by reducing the phosphorylation and transcriptional activity of CREB. Additional ChIP analyses of the *G6Pase* and *Pepck* promoters revealed that FGF15 also reduced PGC-1α binding to these promoters (Fig. 4D and E). Interestingly, FGF15 decreased CREB binding to the *G6Pase* promoter but not the *Pepck* promoter (Fig. 4D and E). The basis for this difference is not known.

To confirm the effect of FGF15/19 on hepatic CREB activity, wild-type mice were infected with an adenovirus containing a CRE-luciferase (luc) reporter (Ad-CREluc) and then administered either vehicle or FGF19. As expected, Ad-CRE-luc-infected mice treated with vehicle showed significant induction of luciferase activity in response to a 6 hr fast (Fig. 4F). This induction of luciferase activity was markedly attenuated in mice treated with FGF19 (Fig. 4F and G). Thus, FGF19 efficiently suppresses hepatic CREB activity *in vivo*.

Discussion

We recently showed that FGF15/19 stimulates glycogen and protein synthesis in liver (Kir et al., 2011). We now show that FGF15/19 represses hepatic gluconeogenesis, TCA cycle flux and fatty acid oxidation. While there is striking overlap in the actions of FGF15/19 and insulin on liver, there are important temporal and mechanistic differences. Insulin is released rapidly from the pancreas following a meal. In our fasting-refeeding experiments, serum insulin concentrations and downstream Akt phosphorylation in liver peaked approximately 15 min after gavage with a high carbohydrate/high fat liquid diet. While we were unable to directly measure circulating FGF15 concentrations, *Fgf15* mRNA levels in ileum and downstream ERK1/2 phosphorylation in liver peaked approximately 1 hr post gavage. Thus, we propose that FGF15 acts subsequent to insulin. Consistent with this hypothesis, serum FGF19 levels increase in humans 2–3 hr following a meal, when bile acid flux increases across the ileum (Lundasen et al., 2006; Walters et al., 2009). We suggest that FGF15/19 provides a mechanism for regulating metabolism in liver after circulating insulin concentrations have dissipated, thereby easing the transition from the fed to the fasted state. The physiologic importance of this pathway is underscored by FGF15-KO and FGFR4-KO mice, which have increased gluconeogenic gene expression under fed conditions and hyperglycemia in response to fasting-refeeding challenge. Moreover, FGF15-KO mice have elevated glucose levels in response to pyruvate/lactate challenge. Interestingly, circulating FGF19 concentrations were recently shown to be negatively correlated with fasting glucose levels and metabolic syndrome in humans (Reiche et al., 2010; Stejskal et al., 2008). Our metabolic flux measurements indicate that FGF15/19 likely contributes to glycemic control in part by suppressing hepatic gluconeogenesis.

We show that FGF15/19 suppresses gluconeogenic gene expression through a pathway distinct from that of insulin. Phosphorylation of CREB at Ser133, which occurs during fasting, causes it to associate with the coactivators P300 and CBP and to induce gluconeogenic gene expression (Chrivia et al., 1993; Gonzalez and Montminy, 1989; Kwok et al., 1994). FGF15/19 has the opposite effect, inhibiting CREB phosphorylation and its recruitment to the *Pgc1α* and *G6Pase* promoters. These data suggest that the effects of FGF15/19 on liver are likely to extend to other processes regulated by CREB. Since FGF19 treatment caused a trend toward reduced hepatic CRTC2 concentrations (Supplemental Fig. S3A), we cannot exclude that this also contributes to FGF15/19-mediated regulation of CREB activity.

It is presently unclear how FGF15/19 signaling causes CREB dephosphorylation. Given that phosphorylation of CREB at Ser133 has a half-life of ~30 min in NIH 3T3 cells (Michael et al., 2000), the rapidity with which CREB is dephosphorylated in liver suggests that FGF15/19 might activate phosphatases. Several CREB phosphatases, including PP1 and PP2A, have been described (Hagiwara et al., 1992; Wadzinski et al., 1993). However, we have not seen changes in PP1 and PP2A activity in liver extracts prepared from mice treated with FGF19 (Supplemental Fig. S3B). A previous study showed that pharmacologic activation of ERK1/2 with an inhibitor of protein phosphatase, Cdc25A, causes rapid CREB dephosphorylation in hepatoma cells through a mechanism involving inhibition of ribosomal S6 kinase (Wang et al., 2003). Although FGF15/19 efficiently activates ERK1/2, it does not

affect ribosomal S6 kinase activity (Kir et al., 2011), indicating that this pathway is unlikely to be relevant to FGF15/19-mediated inhibition of CREB phosphorylation. We also did not detect changes in PKA activity by western blot analysis using a phosphorylated PKA substrate antibody and liver extracts from FGF19-treated mice (Supplemental Fig. S3C). Thus, additional studies will be required to determine how FGF15/19 affects CREB phosphorylation.

Our finding that FGF15/19 represses fatty acid oxidation in isolated liver is surprising in light of our data showing that neither FGF15 nor FGF19 significantly affected hepatic triglyceride levels, and previous studies showing that whole-body fatty acid oxidation and hepatic triglyceride concentrations are decreased by either pharmacologic administration of recombinant FGF19 or its transgenic overexpression (Fu et al., 2004; Tomlinson et al., 2002). A similar paradox was reported in mice lacking FGFR4, the receptor for FGF15/19 in liver: whereas global FGFR4-KO mice were insulin resistant and had increased white adipose tissue mass, they were resistant to diet-induced fatty liver, suggesting that FGFR4 represses hepatic fatty acid catabolism (Huang et al., 2007). These data suggest that the net metabolic profile of FGF15/19 involves effects on additional tissues. In this regard, FGF19-transgenic mice have increased brown adipose tissue mass and thermogenesis (Tomlinson et al., 2002), and injection of recombinant FGF19 into mice activates the FRS2α/ERK1/2 pathway in white adipose tissue (Kurosu et al., 2007). Moreover, intracerebroventricular injection of FGF19 increases metabolic rate (Fu et al., 2004), indicating that FGF19 can act on the central nervous system to mediate some of its effects. The relative contribution of liver versus other tissues to the physiologic and pharmacologic effects of FGF15/19 remains to be determined.

In summary, we show that FGF15/19 inhibits hepatic gluconeogenesis through a pathway involving inhibition of the CREB-PGC-1α signaling cascade. We conclude that FGF15/19 is a late postprandial signal in the temporal cascade of hormones that control hepatic metabolism in response to nutritional status.

Experimental Procedures

Animal experiments

FGF15-KO, FGFR4-KO, SHP-KO, and PGC-1$\alpha^{fl/fl}$ mice were as described (Inagaki et al., 2005; Kerr et al., 2002; Lin et al., 2004; Wright et al., 2004; Yu et al., 2000). Mice were fed standard chow containing 4% fat (Harlan Teklad, #2016). For fasting-refeeding experiments, wild-type, FGF15-KO and FGFR4-KO mice were fasted 24 hr and subjected to a bolus (20 μl/g body weight) of a nutrient rich diet (Ensure, Abbott Laboratories) by oral gavage. Aliquots of tail blood were withdrawn for analysis of glucose, insulin and glucagon levels. Six hr fasting experiments were performed from 6 pm to 12 am unless otherwise specified, and 24 hr fasting experiments were performed from 9 am to 9 am. Insulin tolerance tests were performed by i.p. injection of 0.75 U insulin/kg body weight of insulin into mice following a 4–6 hr fast. All animal experiments were approved by the Institutional Animal Care and Research Advisory Committee of the University of Texas Southwestern Medical Center.

FGF injection experiments

FGF15 and FGF19 were expressed in 911 cells and *E. coli*, respectively, and purified as described (Choi et al., 2006; Inagaki et al., 2005). For the microarray studies, FGF15 and FGF19 were injected into mice intravenously at concentrations of 0.15 μg/g body weight and 1 μg/g body weight, respectively. For all other studies, FGF19 was injected i.p at 1 μg/g.

Adenovirus infections

Control, FGF15, PGC-1α and Cre-recombinase adenovirus injections were performed as described (Inagaki et al., 2005; Lehman et al., 2000). Briefly, 7.5×10^9 particles/g body weight of adenovirus was delivered intravenously by jugular vein injection into 10–14 week old C57BL/6 males (Jackson Laboratories) for FGF15 and PGC-1α overexpression studies, or 12–14 week old PGC-$1\alpha^{fl/fl}$ mice for the Cre-recombinase experiment. Three days after infection of the control, FGF15, PGC-1α adenoviruses, or combination thereof, mice were administered FGF19 or vehicle and fasted for the indicated time. Livers were subsequently isolated and perfused for NMR tracer studies or used for mRNA analysis. For acute, hepatic deletion of PGC-1α, Cre-expressing adenovirus or control adenovirus was administered to PGC-$1\alpha^{fl/fl}$ mice, followed by 9 days of recovery. Mice were then administered vehicle or FGF19, fasted for the indicated time, and livers were subsequently isolated for mRNA analysis.

Ad-CRE-luc activity was measured as described (Dentin et al., 2007). Briefly, 7.5×10^9 particles/g body weight of an adenovirus expressing a cyclic AMP response element (CRE) driving luciferase (Ad-CRE-luc; a gift from Dr. Marc Montminy, Salk Institute) was injected by jugular vein into wild-type 12–16 week old C57BL/6 males. Three days after infection, mice were administered vehicle or FGF19 and then fasted for 6 hr (6 pm to 12 am). In vivo luciferase activity was measured using an IVIS lumina imaging system following luciferin injection, and luciferase activity (photons/second) was normalized to copies of virus DNA infected per liver determined by QPCR analysis of hexon gene expression (Hogg et al., 2010).

In vivo and *ex vivo* tracer studies

Livers from overnight fasted control and FGF15-expressing adenovirus-infected wild-type mice were isolated and perfused for 60 min in a nonrecirculating fashion at 8 ml/min with a Krebs-Henseleit-based perfusion medium as described (Burgess et al., 2003). Ketone and glucose production were determined by standard biochemical assays of the effluent perfusate. Oxygen consumption was determined by oxygen electrode. Relative gluconeogenesis and glycogenolysis were determined using the deuterated water method with deuterium enrichment detected in effluent perfusate glucose by ^{2}H NMR. Relative fluxes through PC/PEPCK and the TCA cycle were determined by ^{13}C isotopomer analysis of effluent perfusate glucose. Relative fluxes were multiplied by absolute hepatic glucose production to determine absolute flux through these pathways.

Pyruvate/lactate challenge experiments were performed by i.p. injection of uniformly labeled pyruvate (1 g/kg mouse; [U-$^{13}C_3$] pyruvate (sodium salt), Cambridge isotopes) and uniformly labeled sodium lactate (2 g/kg mouse; [U-$^{13}C_3$]lactate (sodium salt), Cambridge isotopes) into *ad libitum* fed wild-type and FGF15-KO mice at 8 pm (normal light dark cycle 6 am-6 pm). Pyruvate and lactate were provided together to minimize perturbations of redox state. Twenty minutes prior to treatment, food was removed for the duration of the experiment. Approximately 30 μl of tail blood was then collected at the indicated times and plasma glucose analyzed. Remaining blood was used to measure glucose enrichments by GC-MS as described (Sunny and Bequette, 2010). M+3 was monitored and indicated conversion of pyruvate/lactate to glucose.

Jugular catheters were surgically implanted and the mice were allowed to recover for 5 days. FGF19 was administered by i.p. injection. Twenty min after administration of FGF19, basal endogenous glucose production was determined by steady state infusion of [U-^{13}C]glucose for 90 min, after which blood samples (~50 μl) were collected from the tail vein for isotope dilution analysis of blood glucose by mass spectrometry. At minute 90, a hyperinsulinemic-

euglycemic clamp was initiated after restraining the mice in a tube holder as described (Ayala et al., 2006; Ayala et al.; DeFronzo et al., 1979; Kraegen et al., 1983). Mice were acclimated to the tube holder by daily exposure for 6–8 days prior to the clamp. Briefly, insulin was infused at a constant rate (5 mU/kg/min) together with a variable infusion of 30% glucose solution enriched to 2.5% with [U-^{13}C]glucose to maintain euglycemia. Blood glucose levels were monitored from the tail vein every ten minutes using a glucometer and necessary adjustments to the glucose infusion rate were made to maintain euglycemia. Following 70–80 min of hyperinsulinemic euglycemia to achieve steady state glucose enrichments in the blood, the mice were sacrificed and blood/tissue samples collected and stored at −80°C until analysis. Glucose enrichments were determined by GC-MS as described (Sunny and Bequette, 2010).

Statistical analyses

Statistical analyses were performed as described (Burgess et al., 2007; Inagaki et al., 2007).

Highlights for Potthoff et al

- The intestinal hormone, FGF15/19, inhibits postprandial hepatic gluconeogenesis.
- FGF15/19 is induced after insulin to regulate postprandial hepatic metabolism.
- FGF15/19 suppresses gluconeogenesis by inhibiting the CREB-PGC-1α pathway.

Supplementary Material

Refer to Web version on PubMed Central for supplementary material.

Acknowledgments

We thank Dr. Bruce Spiegelman for the PGC-1α$^{fl/fl}$ mice, Dr. Marc Montminy for the Ad-CRE-luc adenovirus and antibodies, Joao Duarte, Dr. Xunshan Ding and Jessica Mullens for technical assistance, and Xiarong Fu for GC-MS support. This research was supported by the Howard Hughes Medical Institute (D.J.M.), NIH grants DK067158 (S.A.K. and D.J.M), U19DK62434 (D.J.M.), DK078187 (B.N.F.), DK078184 and DK076269 (S.C.B.), and the Robert A. Welch Foundation (I-1275 to D.J.M. and I-1588 to S.A.K.).

References

Ahren B, Havel PJ. Leptin increases circulating glucose, insulin and glucagon via sympathetic neural activation in fasted mice. Int J Obes Relat Metab Disord. 1999; 23:660–665. [PubMed: 10411242]

Ayala JE, Bracy DP, McGuinness OP, Wasserman DH. Considerations in the design of hyperinsulinemic-euglycemic clamps in the conscious mouse. Diabetes. 2006; 55:390–397. [PubMed: 16443772]

Ayala JE, Samuel VT, Morton GJ, Obici S, Croniger CM, Shulman GI, Wasserman DH, McGuinness OP. Standard operating procedures for describing and performing metabolic tests of glucose homeostasis in mice. Dis Model Mech. 2010; 3:525–534. [PubMed: 20713647]

Bhatnagar S, Damron HA, Hillgartner FB. Fibroblast growth factor-19, a novel factor that inhibits hepatic fatty acid synthesis. J Biol Chem. 2009; 284:10023–10033. [PubMed: 19233843]

Bittinger MA, McWhinnie E, Meltzer J, Iourgenko V, Latario B, Liu X, Chen CH, Song C, Garza D, Labow M. Activation of cAMP response element-mediated gene expression by regulated nuclear transport of TORC proteins. Curr Biol. 2004; 14:2156–2161. [PubMed: 15589160]

Burgess SC, He T, Yan Z, Lindner J, Sherry AD, Malloy CR, Browning JD, Magnuson MA. Cytosolic phosphoenolpyruvate carboxykinase does not solely control the rate of hepatic gluconeogenesis in the intact mouse liver. Cell Metab. 2007; 5:313–320. [PubMed: 17403375]

Burgess SC, Leone TC, Wende AR, Croce MA, Chen Z, Sherry AD, Malloy CR, Finck BN. Diminished hepatic gluconeogenesis via defects in tricarboxylic acid cycle flux in peroxisome proliferator-activated receptor gamma coactivator-1alpha (PGC-1alpha)-deficient mice. J Biol Chem. 2006; 281:19000–19008. [PubMed: 16670093]

Burgess SC, Weis B, Jones JG, Smith E, Merritt ME, Margolis D, Dean Sherry A, Malloy CR. Noninvasive evaluation of liver metabolism by 2H and 13C NMR isotopomer analysis of human urine. Anal Biochem. 2003; 312:228–234. [PubMed: 12531210]

Choi M, Moschetta A, Bookout AL, Peng L, Umetani M, Holmstrom SR, Suino-Powell K, Xu HE, Richardson JA, Gerard RD, Mangelsdorf DJ, Kliewer SA. Identification of a hormonal basis for gallbladder filling. Nat Med. 2006; 12:1253–1255. [PubMed: 17072310]

Chrivia JC, Kwok RP, Lamb N, Hagiwara M, Montminy MR, Goodman RH. Phosphorylated CREB binds specifically to the nuclear protein CBP. Nature. 1993; 365:855–859. [PubMed: 8413673]

DeFronzo RA, Tobin JD, Andres R. Glucose clamp technique: a method for quantifying insulin secretion and resistance. Am J Physiol. 1979; 237:E214–E223. [PubMed: 382871]

Dentin R, Liu Y, Koo SH, Hedrick S, Vargas T, Heredia J, Yates J 3rd, Montminy M. Insulin modulates gluconeogenesis by inhibition of the coactivator TORC2. Nature. 2007; 449:366–369. [PubMed: 17805301]

Finck BN, Kelly DP. PGC-1 coactivators: inducible regulators of energy metabolism in health and disease. J Clin Invest. 2006; 116:615–622. [PubMed: 16511594]

Fu L, John LM, Adams SH, Yu XX, Tomlinson E, Renz M, Williams PM, Soriano R, Corpuz R, Moffat B, Vandlen R, Simmons L, Foster J, Stephan JP, Tsai SP, Stewart TA. Fibroblast growth factor 19 increases metabolic rate and reverses dietary and leptin-deficient diabetes. Endocrinology. 2004; 145:2594–2603. [PubMed: 14976145]

Goetz R, Beenken A, Ibrahimi OA, Kalinina J, Olsen SK, Eliseenkova AV, Xu C, Neubert TA, Zhang F, Linhardt RJ, Yu X, White KE, Inagaki T, Kliewer SA, Yamamoto M, Kurosu H, Ogawa Y, Kuro-o M, Lanske B, Razzaque MS, Mohammadi M. Molecular insights into the klotho-dependent, endocrine mode of action of fibroblast growth factor 19 subfamily members. Mol Cell Biol. 2007; 27:3417–3428. [PubMed: 17339340]

Goldman PS, Tran VK, Goodman RH. The multifunctional role of the co-activator CBP in transcriptional regulation. Recent Prog Horm Res. 1997; 52:103–119. discussion 119–120. [PubMed: 9238849]

Gonzalez GA, Montminy MR. Cyclic AMP stimulates somatostatin gene transcription by phosphorylation of CREB at serine 133. Cell. 1989; 59:675–680. [PubMed: 2573431]

Hagiwara M, Alberts A, Brindle P, Meinkoth J, Feramisco J, Deng T, Karin M, Shenolikar S, Montminy M. Transcriptional attenuation following cAMP induction requires PP-1-mediated dephosphorylation of CREB. Cell. 1992; 70:105–113. [PubMed: 1352481]

Handschin C, Spiegelman BM. Peroxisome proliferator-activated receptor gamma coactivator 1 coactivators, energy homeostasis, and metabolism. Endocr Rev. 2006; 27:728–735. [PubMed: 17018837]

Herzig S, Long F, Jhala US, Hedrick S, Quinn R, Bauer A, Rudolph D, Schutz G, Yoon C, Puigserver P, Spiegelman B, Montminy M. CREB regulates hepatic gluconeogenesis through the coactivator PGC-1. Nature. 2001; 413:179–183. [PubMed: 11557984]

Hogg RT, Garcia JA, Gerard RD. Adenoviral targeting of gene expression to tumors. Cancer Gene Ther. 2010; 17:375–386. [PubMed: 20139924]

Holt JA, Luo G, Billin AN, Bisi J, McNeill YY, Kozarsky KF, Donahee M, Wang da Y, Mansfield TA, Kliewer SA, Goodwin B, Jones SA. Definition of a novel growth factor-dependent signal cascade for the suppression of bile acid biosynthesis. Genes Dev. 2003; 17:1581–1591. [PubMed: 12815072]

Huang X, Yang C, Luo Y, Jin C, Wang F, McKeehan WL. FGFR4 prevents hyperlipidemia and insulin resistance but underlies high-fat diet induced fatty liver. Diabetes. 2007; 56:2501–2510. [PubMed: 17664243]

Inagaki T, Choi M, Moschetta A, Peng L, Cummins CL, McDonald JG, Luo G, Jones SA, Goodwin B, Richardson JA, Gerard RD, Repa JJ, Mangelsdorf DJ, Kliewer SA. Fibroblast growth factor 15

functions as an enterohepatic signal to regulate bile acid homeostasis. Cell Metab. 2005; 2:217–225. [PubMed: 16213224]

Inagaki T, Dutchak P, Zhao G, Ding X, Gautron L, Parameswara V, Li Y, Goetz R, Mohammadi M, Esser V, Elmquist JK, Gerard RD, Burgess SC, Hammer RE, Mangelsdorf DJ, Kliewer SA. Endocrine Regulation of the Fasting Response by PPARalpha-Mediated Induction of Fibroblast Growth Factor 21. Cell Metab. 2007; 5:415–425. [PubMed: 17550777]

Kerr TA, Saeki S, Schneider M, Schaefer K, Berdy S, Redder T, Shan B, Russell DW, Schwarz M. Loss of nuclear receptor SHP impairs but does not eliminate negative feedback regulation of bile acid synthesis. Dev Cell. 2002; 2:713–720. [PubMed: 12062084]

Kir S, Beddow SA, Samuel VT, Miller P, Previs SFS, G I, Kliewer SA, Mangelsdorf DJ. FGF15/19 is a postprandial, insulin-independent activator of protein and glycogen synthesis. Science. 2011 *in press*.

Koo SH, Flechner L, Qi L, Zhang X, Screaton RA, Jeffries S, Hedrick S, Xu W, Boussouar F, Brindle P, Takemori H, Montminy M. The CREB coactivator TORC2 is a key regulator of fasting glucose metabolism. Nature. 2005; 437:1109–1111. [PubMed: 16148943]

Kraegen EW, James DE, Bennett SP, Chisholm DJ. In vivo insulin sensitivity in the rat determined by euglycemic clamp. Am J Physiol. 1983; 245:E1–E7. [PubMed: 6346896]

Kurosu H, Choi M, Ogawa Y, Dickson AS, Goetz R, Eliseenkova AV, Mohammadi M, Rosenblatt KP, Kliewer SA, Kuro-o M. Tissue-specific expression of betaKlotho and fibroblast growth factor (FGF) receptor isoforms determines metabolic activity of FGF19 and FGF21. J Biol Chem. 2007; 282:26687–26695. [PubMed: 17623664]

Kwok RP, Lundblad JR, Chrivia JC, Richards JP, Bachinger HP, Brennan RG, Roberts SG, Green MR, Goodman RH. Nuclear protein CBP is a coactivator for the transcription factor CREB. Nature. 1994; 370:223–226. [PubMed: 7913207]

Lehman JJ, Barger PM, Kovacs A, Saffitz JE, Medeiros DM, Kelly DP. Peroxisome proliferator-activated receptor gamma coactivator-1 promotes cardiac mitochondrial biogenesis. J Clin Invest. 2000; 106:847–856. [PubMed: 11018072]

Lin BC, Wang M, Blackmore C, Desnoyers LR. Liver-specific activities of FGF19 require Klotho beta. J Biol Chem. 2007; 282:27277–27284. [PubMed: 17627937]

Lin J, Wu PH, Tarr PT, Lindenberg KS, St-Pierre J, Zhang CY, Mootha VK, Jager S, Vianna CR, Reznick RM, Cui L, Manieri M, Donovan MX, Wu Z, Cooper MP, Fan MC, Rohas LM, Zavacki AM, Cinti S, Shulman GI, Lowell BB, Krainc D, Spiegelman BM. Defects in adaptive energy metabolism with CNS-linked hyperactivity in PGC-1alpha null mice. Cell. 2004; 119:121–135. [PubMed: 15454086]

Lundasen T, Galman C, Angelin B, Rudling M. Circulating intestinal fibroblast growth factor 19 has a pronounced diurnal variation and modulates hepatic bile acid synthesis in man. J Intern Med. 2006; 260:530–536. [PubMed: 17116003]

Mayr B, Montminy M. Transcriptional regulation by the phosphorylation-dependent factor CREB. Nat Rev Mol Cell Biol. 2001; 2:599–609. [PubMed: 11483993]

Michael LF, Asahara H, Shulman AI, Kraus WL, Montminy M. The phosphorylation status of a cyclic AMP-responsive activator is modulated via a chromatin-dependent mechanism. Mol Cell Biol. 2000; 20:1596–1603. [PubMed: 10669737]

Parker JC, Andrews KM, Allen MR, Stock JL, McNeish JD. Glycemic control in mice with targeted disruption of the glucagon receptor gene. Biochem Biophys Res Commun. 2002; 290:839–843. [PubMed: 11785978]

Puigserver P, Spiegelman BM. Peroxisome proliferator-activated receptor-gamma coactivator 1 alpha (PGC-1 alpha): transcriptional coactivator and metabolic regulator. Endocr Rev. 2003; 24:78–90. [PubMed: 12588810]

Reiche M, Bachmann A, Lossner U, Bluher M, Stumvoll M, Fasshauer M. Fibroblast Growth Factor 19 Serum Levels: Relation to Renal Function and Metabolic Parameters. Hormone and Metabolic Research. 2010; 42:178–181. [PubMed: 20013647]

Screaton RA, Conkright MD, Katoh Y, Best JL, Canettieri G, Jeffries S, Guzman E, Niessen S, Yates JR 3rd, Takemori H, Okamoto M, Montminy M. The CREB coactivator TORC2 functions as a calcium- and cAMP-sensitive coincidence detector. Cell. 2004; 119:61–74. [PubMed: 15454081]

Stejskal D, Karpisek M, Hanulova Z, Stejskal P. Fibroblast growth factor-19: development, analytical characterization and clinical evaluation of a new ELISA test. Scand J Clin Lab Invest. 2008; 68:501–507. [PubMed: 18609104]

Sunny NE, Bequette BJ. Gluconeogenesis differs in developing chick embryos derived from small compared with typical size broiler breeder eggs. J Anim Sci. 2010; 88:912–921. [PubMed: 19966165]

Tomlinson E, Fu L, John L, Hultgren B, Huang X, Renz M, Stephan JP, Tsai SP, Powell-Braxton L, French D, Stewart TA. Transgenic mice expressing human fibroblast growth factor-19 display increased metabolic rate and decreased adiposity. Endocrinology. 2002; 143:1741–1747. [PubMed: 11956156]

Wadzinski BE, Wheat WH, Jaspers S, Peruski LF Jr, Lickteig RL, Johnson GL, Klemm DJ. Nuclear protein phosphatase 2A dephosphorylates protein kinase A-phosphorylated CREB and regulates CREB transcriptional stimulation. Mol Cell Biol. 1993; 13:2822–2834. [PubMed: 8386317]

Walters JR, Tasleem AM, Omer OS, Brydon WG, Dew T, le Roux CW. A new mechanism for bile acid diarrhea: defective feedback inhibition of bile acid biosynthesis. Clin Gastroenterol Hepatol. 2009; 7:1189–1194. [PubMed: 19426836]

Wang Z, Zhang B, Wang M, Carr BI. Persistent ERK phosphorylation negatively regulates cAMP response element-binding protein (CREB) activity via recruitment of CREB-binding protein to pp90RSK. J Biol Chem. 2003; 278:11138–11144. [PubMed: 12540838]

Wright TJ, Ladher R, McWhirter J, Murre C, Schoenwolf GC, Mansour SL. Mouse FGF15 is the ortholog of human and chick FGF19, but is not uniquely required for otic induction. Dev Biol. 2004; 269:264–275. [PubMed: 15081372]

Wu X, Ge H, Gupte J, Weiszmann J, Shimamoto G, Stevens J, Hawkins N, Lemon B, Shen W, Xu J, Veniant MM, Li YS, Lindberg R, Chen JL, Tian H, Li Y. Co-receptor requirements for fibroblast growth factor-19 signaling. J Biol Chem. 2007; 282:29069–29072. [PubMed: 17711860]

Yu C, Wang F, Kan M, Jin C, Jones RB, Weinstein M, Deng CX, McKeehan WL. Elevated cholesterol metabolism and bile acid synthesis in mice lacking membrane tyrosine kinase receptor FGFR4. J Biol Chem. 2000; 275:15482–15489. [PubMed: 10809780]

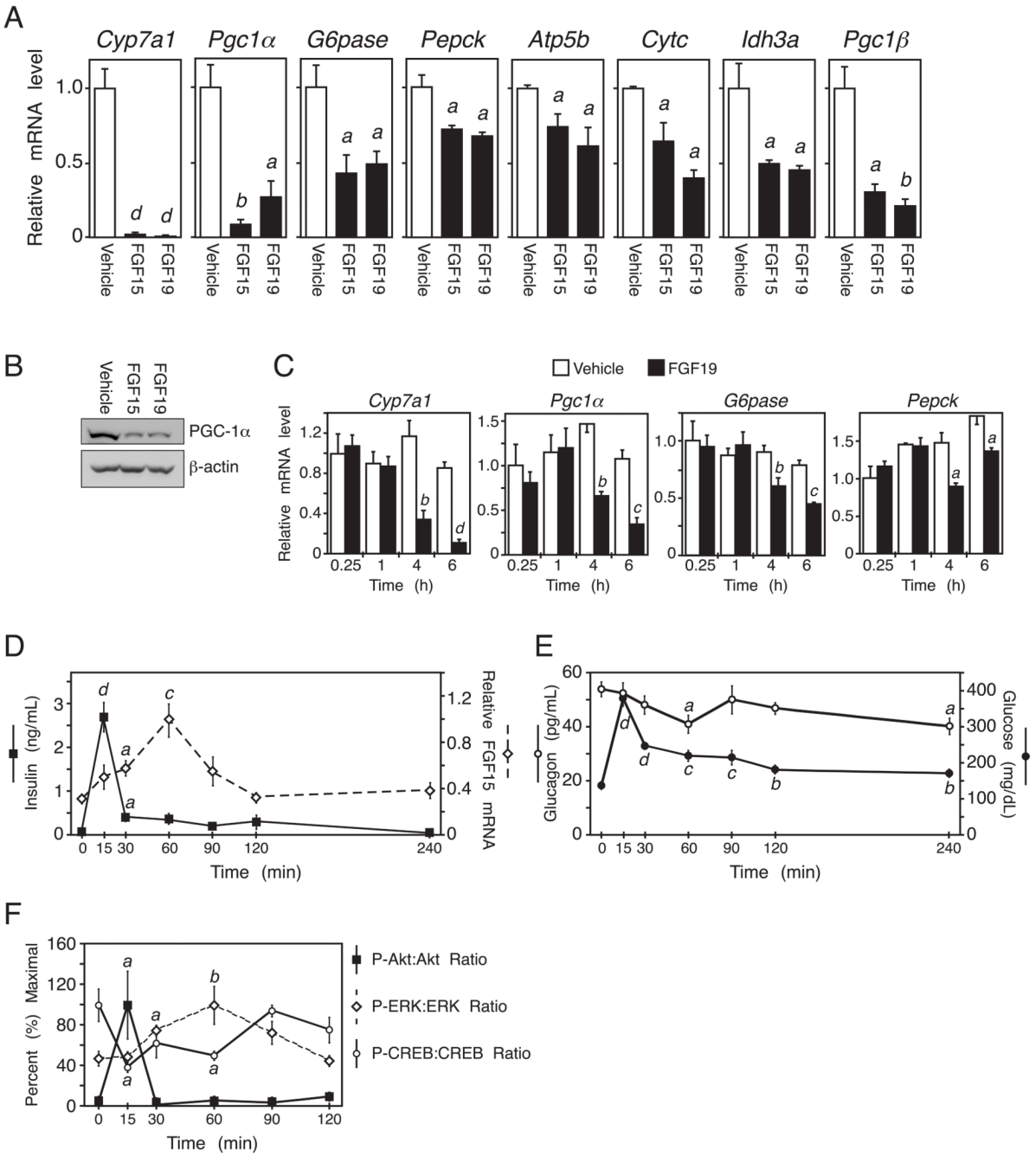

Figure 1. FGF15/19 represses PGC-1α and gluconeogenic gene expression

(A) Hepatic gene expression measured by QPCR in mice treated with vehicle, FGF15 or FGF19 for 6 hr (n = 4/group). Mice were fasted during the treatment period. (B) Western blot analysis of PGC-1α in liver homogenates pooled from groups of 4 mice treated with vehicle, FGF15 or FGF19 as in (A). (C) Hepatic gene expression measured by QPCR in overnight fasted mice injected with FGF19 for the indicated times (n = 4/group). (D) Ileum *Fgf15* mRNA and plasma insulin levels from fasted-refed mice at the indicated times after refeeding (n = 5/group). (E) Plasma glucose and glucagon levels from fasted-refed mice at the indicated times after refeeding (n = 5/group). (F) Quantification of hepatic phospho-Akt/total Akt, phospho-ERK1/2/total ERK1/2, and phospho-CREB/total CREB from fasted-

refed mice at the indicated times after refeeding (n = 4/group). Data are shown as percent of maximal phosphorylation for each protein and represent the mean ± SEM. Different lowercase letters indicate statistical significance (a, $P< 0.05$; b, $P< 0.01$; c, $P< 0.005$; and d, $P< 0.001$ versus control). See also Fig. S1.

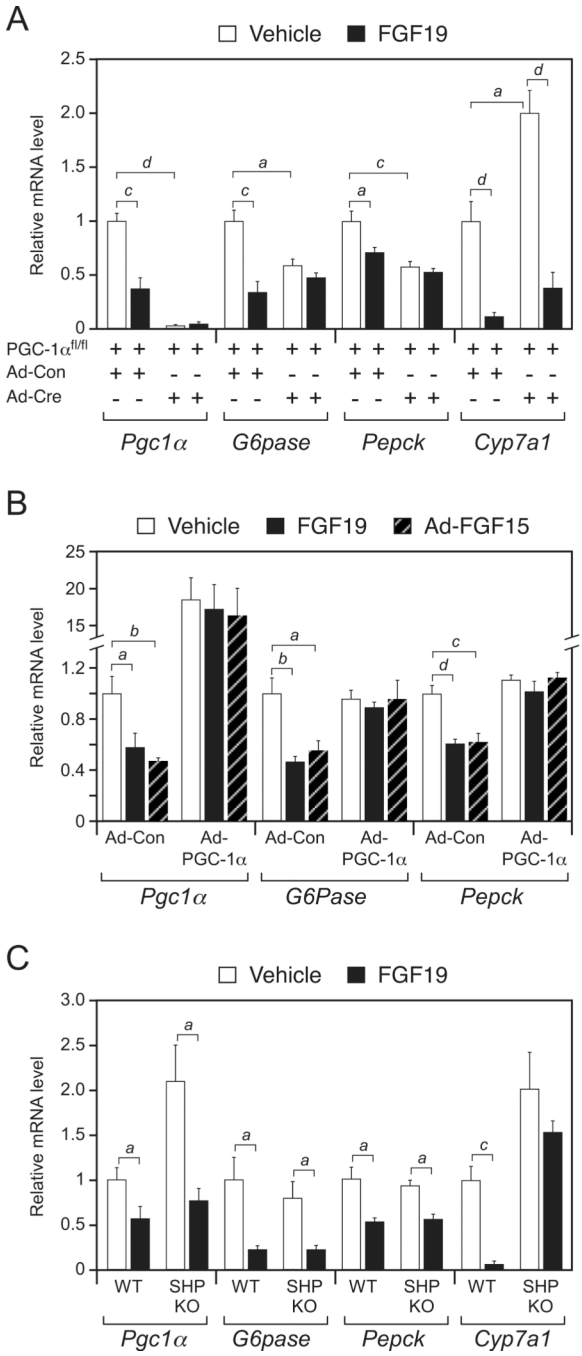

Figure 2. PGC-1α, but not SHP, is required for FGF15/19 regulation of metabolic gene expression

(A) Hepatic gene expression analyzed by QPCR in groups of PGC-1a$^{fl/fl}$ mice administered control (Ad-Con) or Cre-expressing (Ad-Cre) adenovirus and subsequently administered vehicle or FGF19 for 6 hr (n = 5–6/group). Mice were fasted during the treatment period. (B) Hepatic gene expression analyzed by QPCR in groups of wild-type (WT) mice infected with Ad-Con or PGC-1α-expressing adenovirus (Ad-PGC-1α) and subsequently administered vehicle or FGF19 for 6 hr. Mice were fasted during the treatment period. Subgroups of the Ad-Con and Ad-PGC-1α groups were co-administered an FGF15-expressing adenovirus (Ad-FGF15). All mice were fasted during the last 6 hr of the

experiment (n = 5–7/group). (C) Hepatic gene expression analyzed by QPCR in groups of WT and SHP-KO mice administered vehicle or FGF19 for 6 hr (n = 4/group). Mice were fasted during the treatment period. Data are presented as mean ± SEM (*a*, $P < 0.05$; *b*, $P < 0.01$; *c*, $P < 0.005$; *d*, $P < 0.001$).

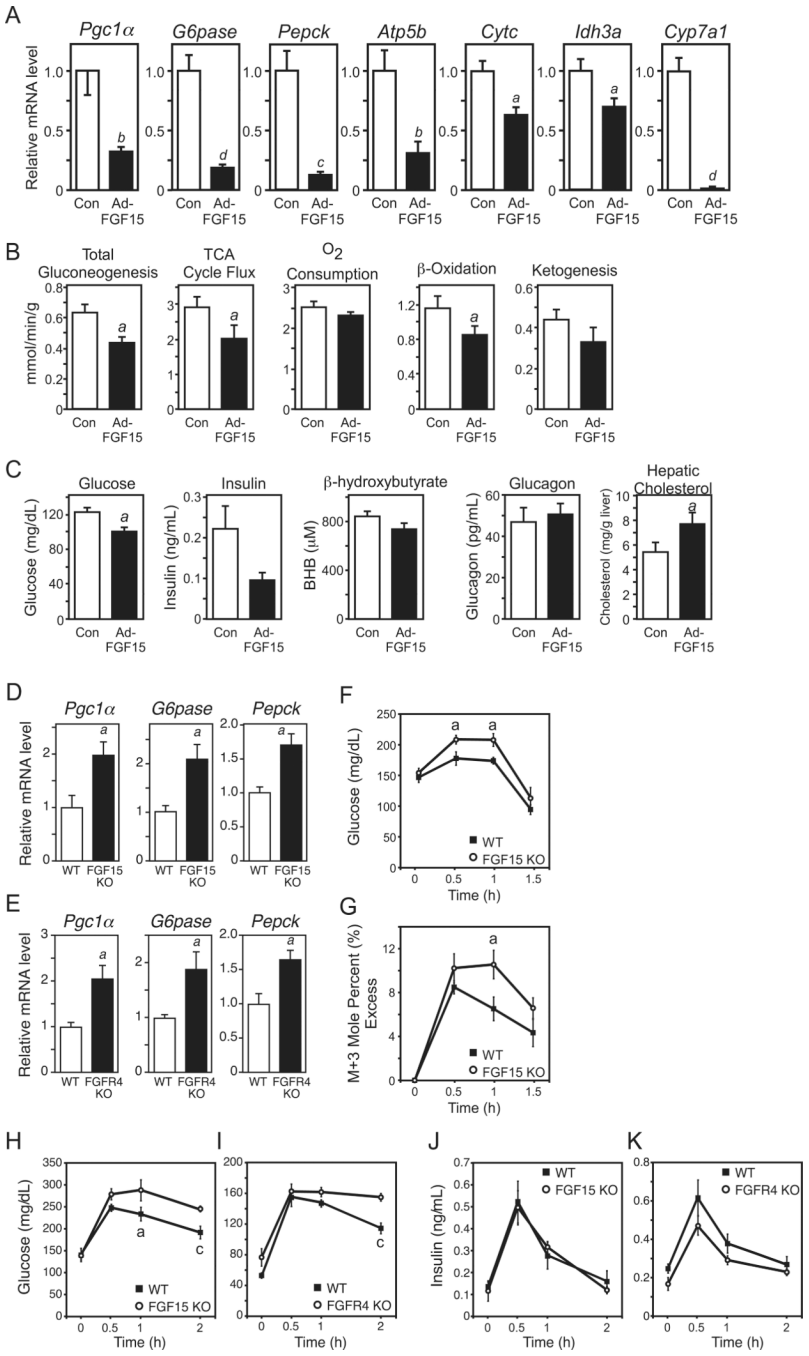

Figure 3. FGF15 represses hepatic gluconeogenesis, TCA cycle flux and fatty acid oxidation

(A) Hepatic gene expression measured by QPCR in mice infected with control (Con) or FGF15-expressing adenovirus (Ad-FGF15) for 3 days and then fasted overnight (n = 5/group). (B) Metabolic pathway flux measured by NMR in perfused livers from mice infected with control or FGF15-expressing adenovirus and fasted as in (A) (n = 8/group). (C) Metabolic parameters in mice infected with control (Con) or FGF15-expressing adenovirus (Ad-FGF15) for 3 days and then fasted for 6 hr (n = 8/group). (D, E) Hepatic gene expression measured by QPCR in fed FGF15-knockout (KO) (D) or FGFR4-KO mice (E) or their wild-type (WT) counterparts (n = 6/group). (F, G) Plasma glucose (F) and mole percent (%) labeled glucose versus unlabeled glucose (G) following a labeled pyruvate/

lactate challenge in WT and FGF15-KO mice (n = 5–6/group). (H–K) Plasma glucose and insulin concentrations in fasted-refed WT, FGF15-KO and FGFR4-KO mice at the indicated times after refeeding (n = 6/group). Data are presented as mean ± SEM (*a*, $P < 0.05$; *b*, $P < 0.01$; *c*, $P < 0.005$; *d*, $P < 0.001$). See also Fig. S2.

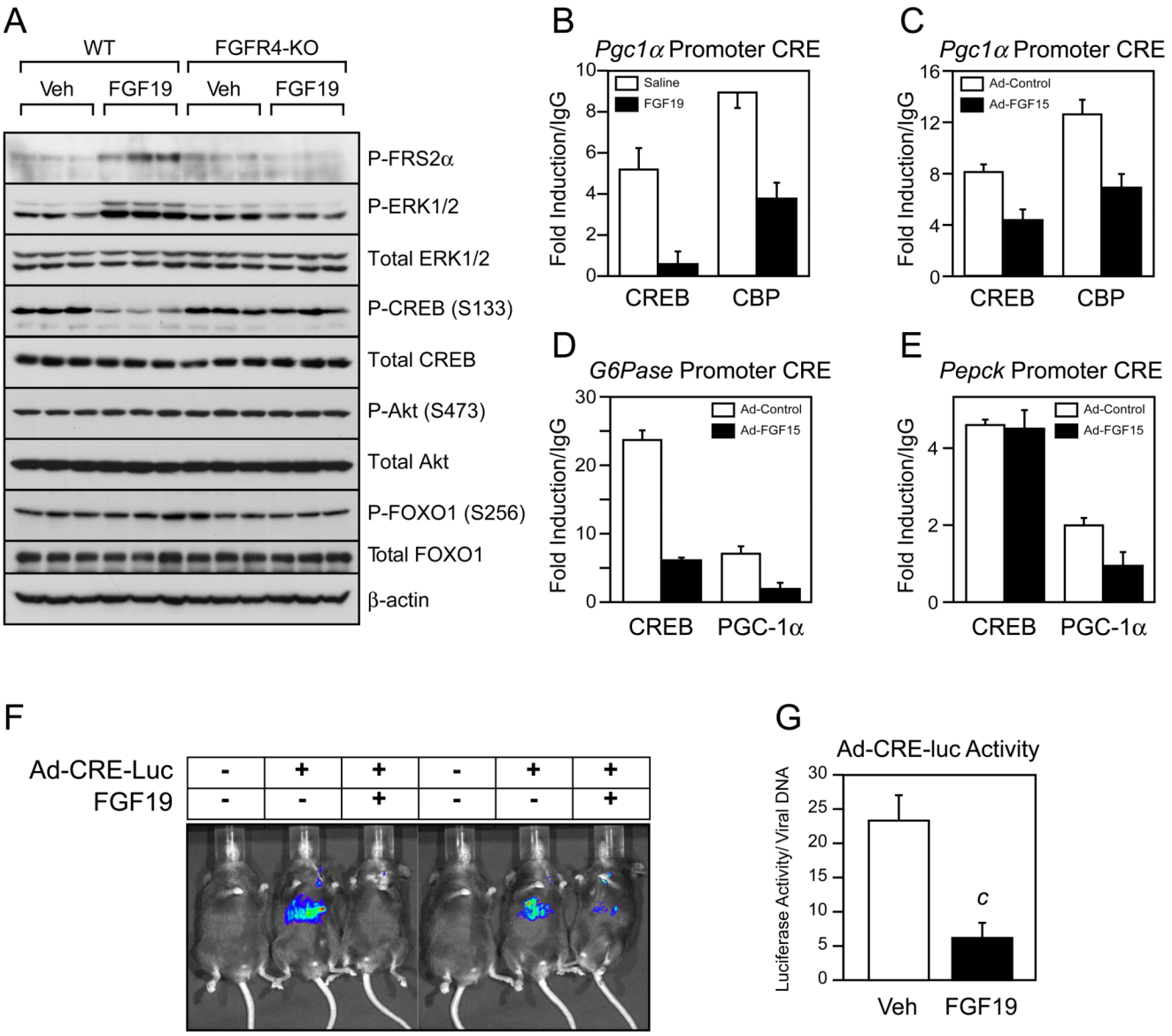

Figure 4. FGF15/19 signaling reduces CREB phosphorylation and activity

(A) Western blot analysis of total and phosphorylated FRS2α, ERK1/2, CREB, Akt, and FOXO1 in liver lysates from individual overnight fasted wild-type (WT) and FGFR4-knockout (KO) mice 30 min after treatment with vehicle or FGF19. β-Actin served as a loading control. (B–E) ChIP analysis of the cyclic AMP response elements (CRE) in the *Pgc1α*, *G6pase*, and *Pepck* promoters using CREB, CBP and PGC-1α antibodies as indicated and pooled liver lysates (three repeats/pool; n = 4/pool of each group). For (B), mice were administered saline or FGF19 for 1 hr and fasted during the treatment period. For (C–E), mice were injected with control or FGF15-expressing adenovirus for 3 days and killed after an overnight fast. (F) Images of luciferase activity in mice infected with a CRE-luciferase reporter (Ad-CRE-luc) or control adenovirus and subsequently treated with vehicle or FGF19 for 6 hr. Mice were fasted during the treatment period. (G) Quantified luciferase activity normalized to the number of virus particles per liver (n = 6/group). All data are presented as mean ± SEM (*c*, $P < 0.005$). See also Fig. S3.